

FRACTAL KOCH MULTIBAND TEXTILE ANTENNA PERFORMANCE WITH BENDING, WET CONDITIONS AND ON THE HUMAN BODY

Mohd E. Jalil, Mohamad K. A. Rahim^{*}, Noor A. Samsuri, Noor A. Murad, Huda A. Majid, Kamilia Kamardin, and Muhamad A. Abdullah

Communication Engineering Department, Faculty of Electrical Engineering, Universiti Teknologi Malaysia, Skudai, Johor 81310, Malaysia

Abstract—A multiband Fractal Koch dipole textile antenna is proposed for wearable applications. The antenna is designed to operate at 0.9 GHz, 2.45 GHz and 5.8 GHz. Denim materials as the substrate are selected aiming to obtain robustness, flexibility and a lightweight textile antenna. The antenna model is designed, simulated, optimized and analyzed using Microwave Studio CST software. Two types of multiband antenna prototypes are fabricated and evaluated with different conducting elements (Shield It fabric and copper foil tape). Antenna performance is observed in terms of return loss, bandwidth, radiation pattern and realized gain. Three different comprehensive analyses are taken into consideration: measurement antenna with different bending sizes, on-body measurement and under wet conditions. The antenna performances are evaluated based on resonant frequency (f_o) and bandwidth (BW). The antennas performance with bending on the human body (arm & forearm) is compared and investigated. A suitable placement on the body has been discovered between the chest and backside. The antennas have also been tested under wet conditions to ensure a stable characteristic under the influence of water.

Received 12 April 2013, Accepted 31 May 2013, Scheduled 26 June 2013

* Corresponding author: Mohamad Kamal A. Rahim (mkamal@fke.utm.my).

1. INTRODUCTION

The advancement of wearable computer system technology has been rapidly growing to enhance the quality and efficiency of life by providing a light-weight and flexible mobile system. Usability, functionality, durability, safety and comfort have become important elements of a wearable system [1]. The system known as “intelligent clothing with sensing, displaying, transmission of information and communication” has been developed in health monitoring activity in the medical sector, surveillance in military units and disease prevention and citizen medicine in =healthcare sector. In medical applications, biomedical smart clothing with multiple sensors have been introduced, such as VTAMN (France) which has been integrated with a breath-rate, temperature and fall/shock biosensor with GSM/GPRS module into the clothes. WEALTHY (Europe) clothes have also been developed to monitor patient activity, to ensure safety and provide reassurance. Life Shirt (USA), a washable smart textile which includes EEG, ECG and blood pressure sensors, is built for cough and respiration monitoring. For military applications, a fibre-optic sensor has been integrated into soldier uniform to detect various hazards such as chemical, biological and thermal ones [2].

In wearable communication systems, the Bluetooth range from 2.4 to 2.48 GHz is widely used for short range data transfer, remote patient monitoring and position tracking in indoor environments. Other short range communications used in wearable applications are Zigbee/IEEE892.15.4 (0.915 and 2.45 GHz) and WIFI (2.4 and 5.8 GHz) [3]. Antenna as a transmitter and receiver is required for the wearable system. In addition, flexible, light-weight, comfortable and robustness are suitable characteristics in designing wearable antenna [4]. Therefore, textile antenna is a strong candidate for wearable applications. The textile antenna features allow for antenna integration with the garment without disrupting the user. Recently, researchers have focused on various designs and materials for wearable textile antenna. For example, washable Ultra-Wide Band (UWB) fully textile antenna with flannel fabric using embroidered technique has been introduced [5]. Denim fabric is also one of the best option materials for designing UWB circular patch antenna [6]. On the other hand, a 5.8 GHz hyper LAN patch full-textile antennas with different radiator shapes using polyester clothing have been implemented for body-wearable applications [7]. A dual-band PIFA antenna (2.45 and 5.8 GHz) using felt substrates was investigated in terms of efficiency, bandwidth and resonant frequency for on-body measurement [8]. A reconfigurable antenna with U-slot patch utilising fabric substrate was

introduced for wrist-wearable applications [9]. Also, flexible UHF RFID printed antennas using paper substrate have been developed for “Green Electronics” [10].

Electromagnetic properties, permittivity, ϵ_r and loss tangent ($\tan \delta$) are the main considerations for determining the substrate. The substrate, which is the crucial part of an antenna, should be formed by material which produces high efficiency and wide bandwidth. Moreover, low permittivity and thickness could reduce surface wave losses and also improve the impedance bandwidth. Various textile materials, such as flannel, felt, denim polyester and cotton, have been used as substrate. The fabric materials have low relative permittivity, ϵ_r between 1.05 and 1.9, while the loss tangent of fabric antenna, $\tan \delta$, ranges from 0.0001 to 0.025. Fabric permittivity depends on the frequency, moisture content, properties of the fabric structure and packing density in the fabric material [11]. Nevertheless, high conductivity, flexible structure and homogenous sheet resistances are required as the conducting element for an antenna such as copper foil tape, Zelt fabric, Pure Copper Polyester Taffeta fabric and Shield It fabric.

Furthermore, the human body in close proximity, the bending effect and the wetness aspect of textile antenna are the main challenges in producing good performance antenna at all times. The antenna should be able to operate well although involving user movement, posture and position. From previous research, there are reports of return loss fluctuations, efficiency degradation, resonant frequency tuning and bandwidth reduction when the antenna is placed on the human body such as the chest, backside, arm and wrist. Hyper bending antenna drastically changes in physical structure causing changes in resonant frequency [12]. At the same time, reliable and washable antenna needs could be improved with wetness aspect condition. Theoretically, wet antenna is capable to disrupt the actual performance of the antenna due to the high dielectric constant of water. However, low moisture regains of material is able to minimize the effect under wet conditions [13].

The design of a multiband fractal Koch dipole antenna using denim materials which resonates at 0.915, 2.45 and 5.8 GHz is described in [14]. Printed dipole antennas are recommended in this work, since the structure is simple with small volume, light weight and low cost. A standard dipole antenna will produce an omnidirectional pattern with linear polarization [15–17]. Omnidirectional patterns are suitable for mobile devices, base stations and smart clothing which require communicating with other mobile radio with uniform coverage for indoor environments. In order to reduce antenna size, fractal Koch

geometry technique is implemented [18]. For example, log periodic Koch fractal antenna is able to reduce size up to 7% for first iteration and up to 26% for series iteration [19]. Koch fractal-slotted rectangular patch could increase the electrical length of the antenna without increasing the antenna overall size [20]. In this paper, a comprehensive analysis of multiband antenna performance with different bendings, on body measurements and under wet conditions, is investigated and presented.

2. DESIGN CONSIDERATIONS

2.1. Fabric Characterization

Many techniques are available to determine the characteristics of permittivity and loss tangent for semi-solid material such as the Cavity Perturbation method, Mom-segment method, Resonance method, Transmission line and Open Ended Coaxial Probe method. In this paper, the open ended coaxial probe method is chosen to determine the permittivity denim sample with good accuracy and fast measurement. The calibration set-up at the tip probe is conducted by measuring the permittivity of the standard material (air and de-ionized water as a reference liquid). Then, the tip of the probe is pressed on the denim sample with a thickness of 0.8 mm while the S_{11} parameter is measured using a network analyzer. The frequency range is between 300 kHz and 6 GHz. Agilent software is connected with the network analyzer which provides the real part, ϵ'_r , and imaginary part, ϵ''_r , of relative permittivity of material. The relative permittivity of the denim jeans is 1.7 and loss tangent 0.085, respectively. Fig. 1 shows the coaxial probe, permittivity and loss tangent results of the denim textile material.

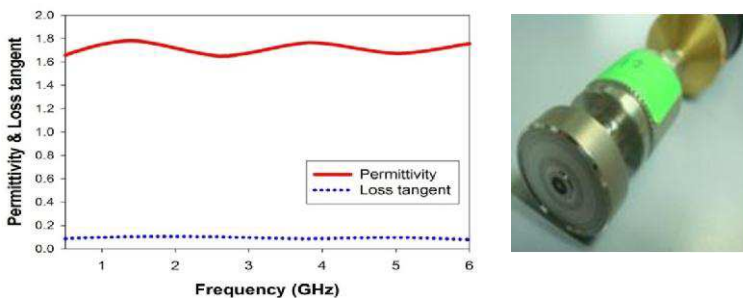


Figure 1. Denim material characterization using the coaxial probe method.

Effective permittivity is required to determine the actual dipole length of the antenna. Calculation of effective permittivity using a close-form method, which depends on the gap between dipole and thickness of substrate, could be more accurate than conventional methods [21]. The formulae for these methods are as follows;

$$\epsilon_{eff} = 1 + \left(\frac{\epsilon_r - 1}{2} \right) \frac{K_2}{K_1} \tag{1}$$

$$K_1 = K(k_1) / K'(k_1) \tag{2}$$

$$K_2 = K(k_2) / K'(k_2) \tag{3}$$

ϵ_r : relative permittivity of substrate.

When $l_{ed} > h$ and $l_{ed} \gg s$, the values of k_1 and k_2 can be approximated by

$$k_1 = \frac{l_{ed}}{l_{ed} + 2s} \tag{4}$$

$$k_2 = e^{-\pi s / (2h)} \tag{5}$$

l_{ed} : the dipole length estimation, s : the gap between dipole arm, h : the thickness of substrate.

2.2. Antenna Design Consideration

Initial design of the straight multiband dipole antenna is shown in Fig. 2. Two quarter wavelength elements are placed back to back with a total length of $\lambda/2$ to form a dipole antenna on the substrate. Koch fractals for the 1st iteration are implemented into the design to reduce the size of antenna without performance degradation. The size is reduced using fractal Koch technique as shown in Fig. 3. The feed is located at the edge of the antenna by using micro strip line feeding technique. From the dipole antenna with Fractal Koch formula, the

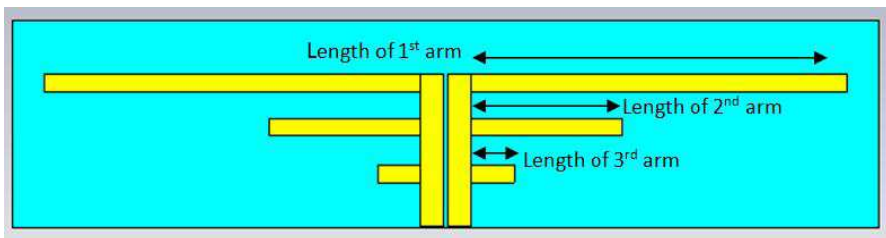


Figure 2. Initial design; straight multiband dipole antenna.

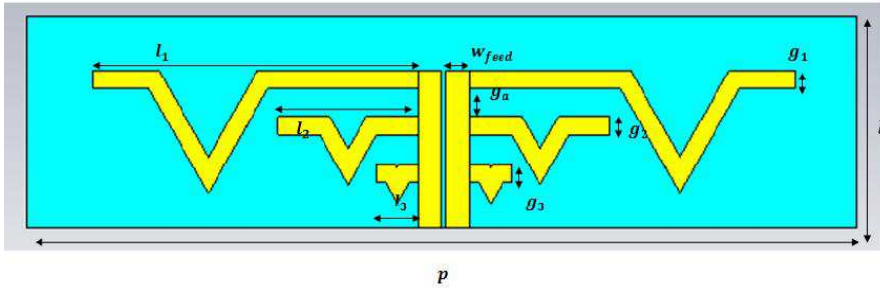


Figure 3. Fractal Koch multiband textile antenna.

total length is determined by;

$$l_o = \frac{3 \times 10^8}{2f \sqrt{\varepsilon_{eff}}} \quad (6)$$

$$l_f = l_o \left(\frac{2 + \cos \phi}{3} \right) \quad (7)$$

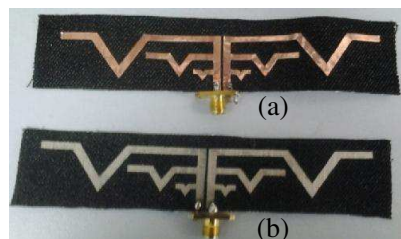
where l_o is the length of conventional dipole antenna, ε_{eff} the effective dielectric constant, and ϕ the degree of flare angle. The optimization of the dimensions is done using CST Microwave software. The miniaturized first arm length, l_1 , of 54.9 mm resonates at 0.915 GHz. The miniaturized second arm length, l_2 , of 23.7 mm and the miniaturized third arm length, l_3 , of 7.05 mm resonate at 2.45 GHz and 5.8 GHz, respectively. The gap between dipole arms, g_a , of 5 mm will minimize the coupling effect between the dipole arms. The height of feed line, h , is 26 mm, the width of feed line, w_{feed} , 3 mm, the width of the first dipole arm, w_1 , 3 mm, the width of the second dipole arm, w_2 , 2.5 mm, and the width of the third dipole arm, w_3 , 2 mm. The total dimension of Fractal Koch textile antenna is 31.1 mm \times 131.2 mm with 60° flare angle. 50 ohm impedance matching of the antenna is obtained by tuning the gap between dipole sides, g_{side} to 0.05 mm, as well as the width of the feed line. In this work, the balun is not considered because the inner conductor of the coaxial with certain length will act as the third arm of the radiator. The balun is needed to prevent radiation from the third arm. But in this case, the feed is matched, and the inner conductor of the coaxial that fed the dipole arm is short enough, so balun is not required. Fig. 3 shows the design layout of Fractal Koch multiband textile antenna. Table 1 shows the optimized value result for the total length of straight dipole and fractal dipole arm.

Table 1. Optimized result for the length of straight dipole arm at 0.915 GHz, 2.45 GHz and 5.8 GHz.

Frequency (GHz)	Optimized Total Straight length (mm) (0th iteration)	Miniaturized Total Fractal Length (mm) (1st iteration)	Reduction in Length (ML) (%)
0.915	129.00	109.8	-14.8%
2.45	56.4	48.9	-13.3%
5.8	15.3	14.4	-5.8%

2.3. Fabrication

High conductivity, coupled with flexible and inelastic mechanical properties, are indispensable aspects in constructing conducting elements for textile antenna. Shield It fabric and copper foil tape have been chosen to compare the antenna performance with different conductive materials. First material, Shield It fabric, weighing 230 g/m^3 , consists of nickel and copper with a woven polyester fabric coating, and hot melts adhesive backing has been used. The estimated conductivity and thickness of Shield It fabric are discovered as $1.18 \times 10^5\text{ S/m}$ and 0.17 mm , respectively. On the other hand, the conformable copper foil with conducting adhesive thickness of 0.11 mm and conductivity of $5.88 \times 10^7\text{ S/m}$ have been used. Low resistivity, inversely proportional to high conductivity, will minimize the electrical losses and thus increase antenna efficiency. In terms of conductivity, copper foil is highly recommended but has a lack of durability and elasticity of material compared with the conducting fabric. Another issue is that the manual fabrication technique using hand works is not recommended because this will generate large errors from the desired dimension. Therefore, cutting machines are introduced to

**Figure 4.** Prototype of textile antenna; (a) copper foil tape and (b) Shield It fabric.

ensure the accuracies of the dimension of the antenna structure. Both conducting textiles, Shield It fabric and copper foil tape, are cut using the machines. Then, the conducting textile is placed on a denim material using a press steamer to ensure strong attachment with the substrate material and minimize the air gap between the substrate and the conductive textile. Lastly, the textile antenna is connected with SMA port by soldering technique. Fig. 4 shows the prototypes of fabricated textile antennas with copper tape and Shield it fabric.

3. RESULTS AND DISCUSSION

3.1. Measurement Results

In this investigation, multiband designs with different conducting materials are presented. The first prototype is designed with copper foil tape (CT antenna), while the second prototype is designed with Shield It fabric (SI antenna). Two prototypes of antennas are tested to evaluate the antenna performance, prior to further investigations. From Fig. 5, the simulated reflection coefficient (S_{11}) shows a similar trend with measurement in free space. However, both measurement results show the resonant frequency, f_o , slightly shifted down at the second and third bands — probably due to the imprecise fabrication and complexity determining the permittivity of substrate. In simulation, CT antenna produces 60 MHz of bandwidth, (BW), while SI antenna produces 110 MHz of BW at the 1st band (f_o ; $CT = 0.90$ GHz, $SI = 0.88$ GHz). For the 2nd band, CT antenna

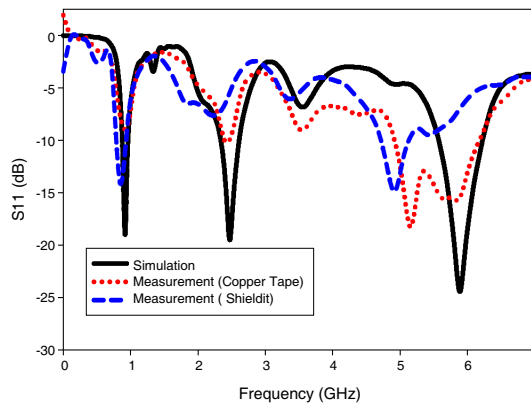


Figure 5. Measured S_{11} of the antenna for the first band (0.915 GHz), the second band (2.45 GHz) and the third band (5.8 GHz).

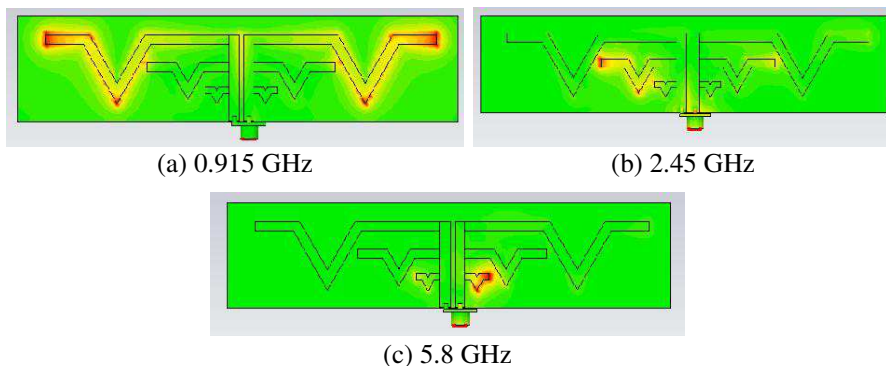


Figure 6. Current distribution at three different frequency band (0.915 GHz, 2.45 GHz and 5.8 GHz).

which provides 10 MHz of BW resonates at 2.44 GHz, while SI antenna resonates at 2.21 GHz. For the 3rd band, CT antenna with 1.26 GHz of BW resonates at 5.16 GHz, and SI resonates with 0.42 GHz of BW at 4.88 GHz which produces the highest BW among all bands. Fabricated CT antennas show better performance than SI antenna. Fig. 6 shows the current distribution of the antenna. The strong current distribution occurs at the longest arm of the dipole antenna which is resonated at 0.915 GHz. The same phenomena occur for high frequency which is at the shortest arm of the antenna at frequency 5.8 GHz.

Simulated and measured radiation patterns of textile antenna using copper tape and Shield It fabric at H -plane and E -plane are presented. Three different samples of radiation pattern at 0.915 GHz, 2.45 GHz and 5.8 GHz for both antennas are achieved. Good agreements between simulated and measured radiation patterns have been shown in Fig. 7. Omni-radiation pattern is produced at the 1st and 2nd bands, while the near omnidirectional pattern is produced for the 3rd band. The gain of the textile antenna at 0.915 GHz, 2.45 GHz and 5.8 is demonstrated in Table 2. From Table 2, CT antenna has better gain than SI antenna at all frequency bands due to its conductivity and the structure of conductive material.

3.2. Bending Experiment

Antenna performance in terms of f_o and BW are investigated under different bending conditions, as shown in Fig. 8. Firstly, CT and SI antennas are bent with horizontal position using cylindrical polystyrenes ($\epsilon_r \cong 1$) with different circumferences, c , 24 cm and 32 cm.

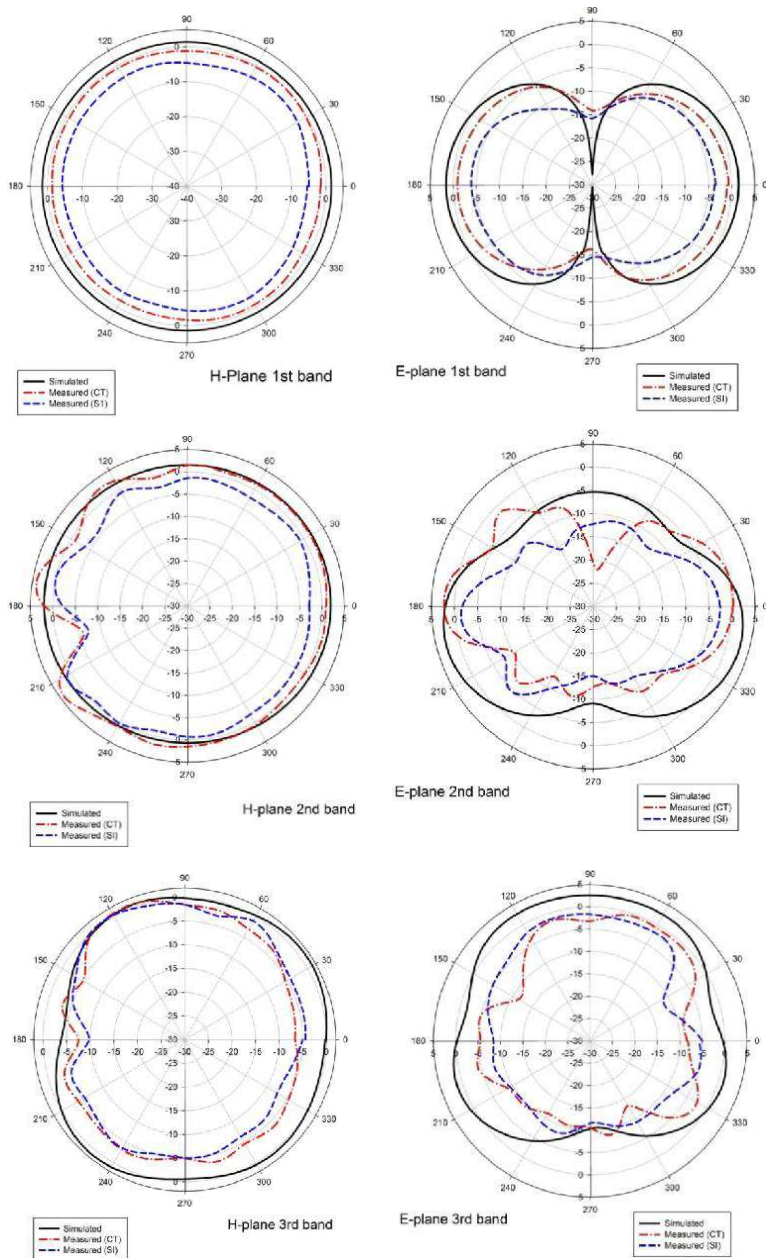


Figure 7. Simulated and measured radiation pattern of the antenna at the first band (0.915 GHz), the second band (2.45 GHz) and the third band (5.8 GHz).

Table 2. Measured S_{11} realized gain of the antenna for first band (0.915 GHz), the second band (2.45 GHz) and the third band (5.8 GHz) with different conducting material.

Frequency	0.915 GHz	2.45 GHz	5.8 GHz
SI antenna (dBi)	-2.63	0.84	0.75
CT antenna (dBi)	0.02	3.20	0.59

Table 3. Measured S_{11} plots of the CT and SI antenna bent with different condition.

Antenna	Parameter (GHz)	Band	Bending				
			Free	Without Body		With Body	
				24 cm	32 cm	23.5 cm	28 cm
CT	BW	1st	0.04	0.01	0.01	0.12	0.14
		2nd	0.09	0.07	-	-	0.32
		3rd	1.24	1.16	1.10	2.80	1.66
	f_o	1st	0.90	0.91	0.91	0.49	0.52
		2nd	2.45	2.45	2.47	1.16	1.32
		3rd	5.16	5.20	5.24	3.03	3.51
SI	BW	1st	0.11	0.01	0.08	0.20	0.17
		2nd	-	-	-	0.28	0.23
		3rd	0.42	0.48	0.46	0.98	0.92
	f_o	1st	0.85	0.85	0.86	0.51	0.60
		2nd	2.24	2.26	2.24	1.23	1.04
		3rd	4.92	4.92	4.86	3.09	3.19

Secondly, both antennas are bent at two curved parts of the body, arm position ($c = 23.5\text{ cm}$) and forearm ($c = 28\text{ cm}$). Figs. 9 and 10 show the S_{11} measurement result for bending conditions of two different types of conductive antenna. The measured f_o and BW of the bent antenna, with and without the body, are compared to the planar antenna and shown in Table 3. From Table 3, the reflection coefficient of SI antenna exhibits average of f_o at 0.86 GHz for the 1st band, 2.25 GHz for the 2nd band and 4.89 GHz for the 3rd band, respectively, while CT antenna resonates at 0.91 GHz, 2.46 GHz and 5.2 GHz, when the antenna is bent without the human body. It is observed that the placement of bent antenna without human body has

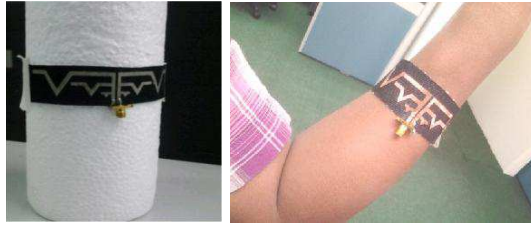


Figure 8. Textile antennas are bent with polystyrene cylinder and arm.



Figure 9. Measured S_{11} plots of the CT antenna bending with different diameter.

minor effect on f_o and BW. However, f_o has been shifted drastically to lower frequency, which averages $f_o = 0.56$ GHz, 1.14 GHz and 3.14 GHz for SI antenna and averages $f_o = 0.51$ GHz, 1.24 GHz and 3.27 GHz for CT antenna, when the antennas are bent on the human body. Initially, the bent antenna with small circumference will shift down f_o due to increment of the antenna resonant length. f_o at high frequency gives significant impact compared to the low frequency under bent condition on human body.

3.3. On-body Measurement

When the antennae are placed on the human body, the performance is strongly influenced due to the electromagnetic coupling of and specific absorption by the body [22]. High permittivity and conductivity of human tissue body will affect the performance and propagation loss of antenna [23]. Therefore, suitable placement of antenna is investigated to find the location with minimum degradation in terms of bandwidth

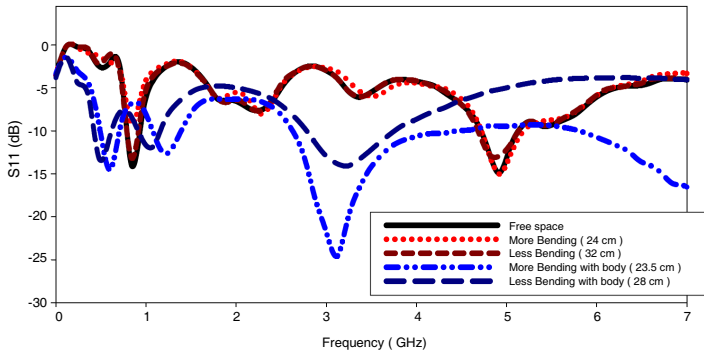


Figure 10. Measured S_{11} plots of the SI antenna bending with different condition.

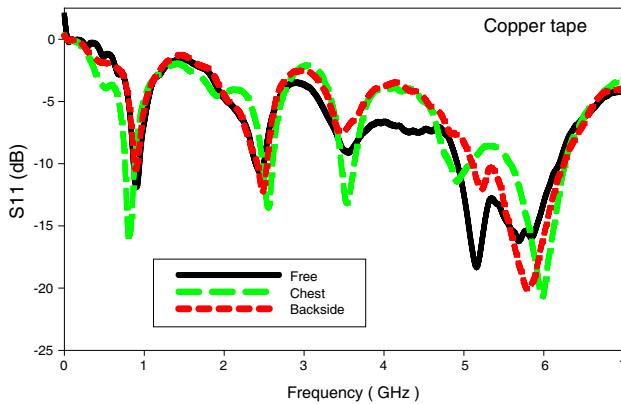


Figure 11. Measured S_{11} plots of CT antenna with different position on human body.

and return loss. Flat and wide body placement is suggested to avoid bending effect, as described in the previous section. Therefore, two placements of antenna, at chest (C) and backside (B), are tested. At the first location, the antennas are placed at the upper backside, which is 18 cm from the neck. At the second location, the antennas are located on the centre of chest which is 15 cm from the neck. A male model worn a cotton shirt with a weight of 67 kg and height of 163 cm is used in the measurement. Both antennas are attached on the shirt (against the human body) in the horizontal orientation.

Due to the coupling body effect, resonance frequency, f_o , of the antenna on the chest body has shifted between -0.06 and 0.10 GHz at the 1st band, $+0.03$ and $+0.13$ GHz at the 2nd band and -0.06 and

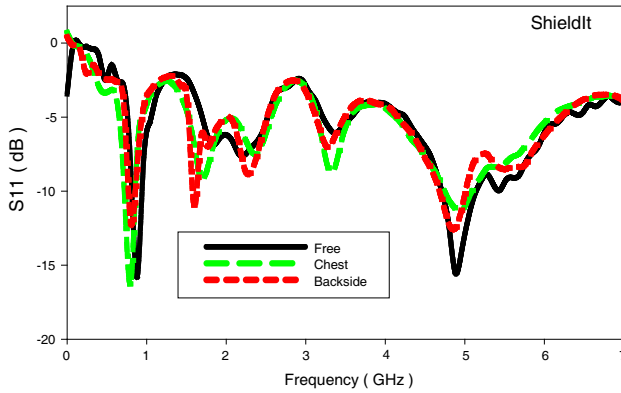


Figure 12. Measured S_{11} plots of SI antenna with different position on human body.

+0.84 GHz at the 3rd band as shown in Fig. 11. Compared with the chest placement in Fig. 12, the backside body has less changed f_o by -0.05 and $+0.02$ GHz for the 1st band, $+0.03$ GHz and $+0.04$ GHz for the 2nd band and $+0.01$ and $+0.64$ GHz for the 3rd band. Moreover, BW of both antennas with backside placement seems similar to the BW of both antennas in free space, as shown in Table 4. Therefore, the backside body is suitable for the best antenna placement on human body.

3.4. Wet Condition Experiment

Antenna performance under wet conditions has to be taken into consideration for designing textile antenna. It is well known that the presence of water with high dielectric constant strongly influences the relative permittivity of substrate. From the previous research, the textile antenna does not work when placed in the water [24, 25]. Therefore, it is important to choose a suitable substrate with low absorption to ensure that the antenna can perform well under wet conditions. Resonant frequency f_o is determined, since it is related to relative permittivity ϵ_r of the substrate. Fig. 13 shows the snapshot of wetness testing on the textile antenna under room temperature. In this analysis, denim material is selected as the substrate of antenna. First of all, the antenna is left immersed in the water until saturation is achieved. The actual mass of the antenna (not including SMA port) is 3.87 g, as recorded by using digital scales before it is immersed into water. After the immersion, the mass of antenna increases to 5.81 g (50% from actual mass). The textile antenna is left to dry while the

Table 4. Measured S_{11} plots of SI antenna with different position on human body.

Antenna	Parameter (GHz)	Band	Free Space	Human Body	
				Chest	Backside
CT	BW	1st	0.04	0.12	0.05
		2nd	0.09	0.12	0.11
		3rd	1.16	0.68	1.12
	f_o	1st	0.90	0.80	0.88
		2nd	2.45	2.56	2.48
		3rd	5.16	6.00	5.80
SI	BW	1st	0.11	0.12	0.08
		2nd	-	-	0.05
		3rd	0.42	0.36	0.32
	f_o	1st	0.85	0.79	0.80
		2nd	2.24	2.37	2.28
		3rd	4.92	4.86	4.93



Figure 13. Antenna are tested under wet conditions.

readings are recorded for 100, 75, 50, 25 and 0% of water absorption based on the current mass. Fig. 14 shows the measurement result of return loss (S_{11}) when the antenna is dried and in wet condition. The water absorption formula is described below:

$$\text{Water Absorption, WA (\%)} = \frac{\text{Current mass} - \text{Dry mass}}{\text{Saturated mass} - \text{Dry mass}} \times 100\% \quad (8)$$

From Table 5, f_o of wet antenna are dropped by 26% at the 1st band, 39% at the 2nd band and 43% at the 3rd band, when the textile antenna is 100% fully wet. Definitely, wet textile antenna enables

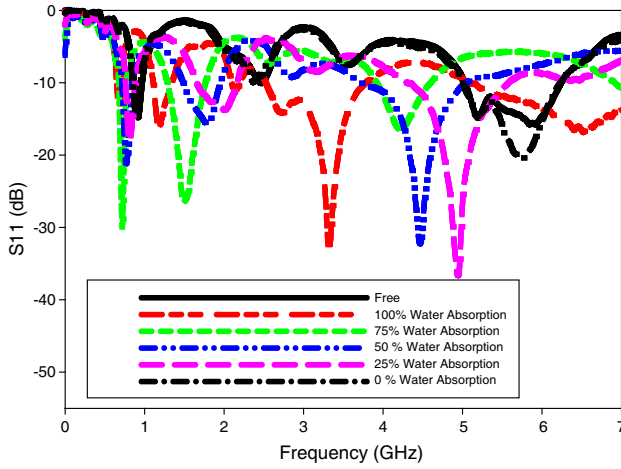


Figure 14. Measured S_{11} plots of the antenna with different % of WA.

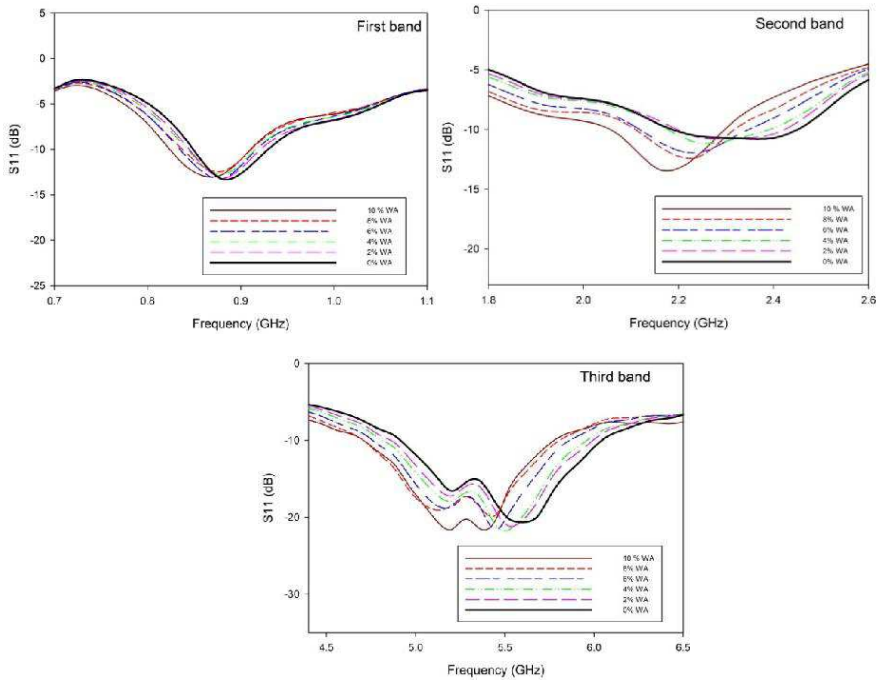


Figure 15. Measured S_{11} plots of the antenna for 1st band, 2nd band and 3rd band with different percentage of water absorption.

Table 5. Measured resonance frequencies of the antenna at different percentage of water absorption.

Amount of WA %	f_o of 1st band (GHz)	f_o of 2nd band (GHz)	f_o of 3rd band (GHz)	Antenna weight (g)
Free space	0.920	2.46	5.84	3.87
100	0.680	1.50	3.31	5.81
75	0.712	1.79	4.21	5.33
50	0.768	2.00	4.46	4.84
25	0.810	2.14	4.93	4.36
0	0.940	2.36	5.59	3.85

Table 6. Measured S_{11} plots of the antenna using with different percentages of water absorption.

Amount of WA %	1st band		2nd band		3rd band	
	f_o (GHz)	BW (GHz)	f_o (GHz)	BW (GHz)	f_o (GHz)	BW (GHz)
10%	0.88	0.090	2.17	0.246	5.38	1.04
8%	0.88	0.086	2.23	0.208	5.43	1.11
6%	0.88	0.097	2.24	0.231	5.45	1.07
4%	0.88	0.089	2.26	0.219	5.50	1.15
2%	0.88	0.095	2.30	0.232	5.54	1.11
0%	0.88	0.094	2.36	0.253	5.59	1.14

the permittivity of denim material to alter to higher value. However, f_o of 100% fully dried antenna gives almost the same value of f_o for free space antenna. A small deviation has been observed between f_o before and after the immersion process of antenna, 2.1% at the 1st band, 4.1% at the 2nd band and 4.2% at the 3rd band. Next, the minimum percentage of WA for a stable characteristic of the antenna is determined for each band. From Figure 15, the antennas require less than 10% of WA at the 1st and 3rd bands in order to maintain good performances of the antenna. However, the antenna requires less than 2% of WA at the 2nd band. From 0 to 10% of WA, the BW is not changed much in the range of 0.086 to 0.09 GHz at the 1st band, 0.208 to 0.253 GHz at the 2nd band and 1.04 to 1.15 GHz at the 3rd band, as shown in Table 6.

4. CONCLUSIONS

In this work, a novel, miniaturized, triple-band first iteration fractal Koch textile dipole antenna, using denim material for wearable applications, has been thoroughly evaluated. It has been shown that the degradation of antenna performances, due to bending conditions on body measurement and wetness aspects, is caused by the shifting of the resonant frequency and bandwidth fluctuations. The suitable placement for the designed antenna is discovered at the backside area of the human body. Good performance is observed when the textile antennas is less than 2% of water absorption. Lastly, the performance of copper tape (CT) antenna is shown to be more profound than Shield It (SI) antenna in terms of return loss, radiation pattern and gain due to the conductivity of the material.

ACKNOWLEDGMENT

The authors would wish to thank the Ministry of Higher Education (MOHE) Research Management Centre (RMC) and Communication Engineering Department, Universiti Teknologi Malaysia (UTM) for the supports of this project under grant Nos. 74578, Q.J130000.7123.02H02 and Q.J130000.7123.04J0

REFERENCES

1. Cho, G., S. Lee, and J. Cho, "Review and reappraisal of smart clothing," *International Journal of Human-computer Interaction*, Vol. 25, No. 6, 2009.
2. Axisa, F., P. M. Schmitt, C. Gehin, G. Delhomme, E. McAdams, and A. Dittmar, "Flexible technologies and smart clothing for citizen medicine, home healthcare, and disease prevention," *IEEE Transactions on Information Technology in Biomedicine*, Vol. 9, No. 3, 325–336, Sep. 2005.
3. Khan, J. Y. and M. R. Yuce, "Wireless body area network (WBAN) for medical applications," *New Development in Biomedical Engineering*, Ch. 31, 2010.
4. Roh, J.-S., Y.-S. Chi, and T. J. Kang, "Wearable textile antenna," *International Journal of Fashion Design, Technology and Education*, No. 3, Vol. 3, 2010.
5. Osman, M. A. R., M. K. Abd Rahim, N. A. Samsuri, H. A. M. Salim, and M. F. Ali, "Embroidered fully textile

- wearable antenna for medical monitoring applications,” *Progress In Electromagnetics Research*, Vol. 117, 321–337, 2011.
6. Osman, M. A. R., M. K. Abd Rahim, M. Azfar, N. A. Samsuri, F. Zubir, and K. Kamardin, “Design, implementation and performance of ultra-wideband textile antenna,” *Progress In Electromagnetics Research B*, Vol. 27, 307–325, 2011.
 7. Sankaralingam, S. and B. Gupta, “Experimental results on Hiperlan/2 antennas for wearable applications,” *Progress In Electromagnetics Research C*, Vol. 25, 27–40, 2012.
 8. Soh, P. J., S. J. Boyes, G. A. E. Vandenbosch, Y. Huang, and S. L. Ooi, “On-body characterization of dual-band all-textile PIFA,” *Progress In Electromagnetic Research*, Vol. 129, 517–539, 2012.
 9. Kim, J.-Y., S.-J. Ha, D. Kim, B. Lee, and C. W. Jung, “Reconfigurable beam steering antenna using U-slot fabric patch for wrist-wearable applications,” *Journal of Electromagnetic Waves and Applications*, Vol. 26, Nos. 11–12, 1545–1553, 2012.
 10. Amin, Y., Q. Chen, L.-R. Zheng, and H. Tenhunen, “Development and analysis of flexible UHF RFID antennas for ‘Green’ electronics,” *Progress In Electromagnetics Research*, Vol. 130, 1–15, 2012.
 11. Salvado, R., C. Loss, R. Gonçalves, and P. Pinho, “Textile materials for the design of wearable antennas: A survey,” *Sensors Journal*, Vol. 12, 15841–15857, 2012.
 12. Sankaralingam, S. and B. Gupta, “Development of textile antennas for body wearable applications and investigations on their performance under bent conditions,” *Progress In Electromagnetics Research B*, Vol. 22, 53–71, 2010.
 13. Hertleer, C., A. Van Laere, H. Rogier, and L. Van Langenhove, “Influence of relative humidity on textile antenna performance,” *Textile Research Journal*, Vol. 80, 177–183, 2010.
 14. Jalil, M. E., M. K. A. Rahim, and N. A. Samsuri, “Multiband antenna at ISM band using textile material,” *IEEE Antennas and Propagation Society International Symposium (APSURSI)*, 1–2, 2012.
 15. Abu, M. and M. K. A. Rahim, “Triple-band printed dipole tag antenna for RFID,” *Progress In Electromagnetics Research C*, Vol. 9, 145–153, 2009.
 16. Fan, Z., S. Qiao, J. T. Huang-Fu, and L.-X. Ran, “A miniaturized printed dipole antenna with V-shaped ground for 2.45 GHz RFID readers,” *Progress In Electromagnetics Research*, Vol. 71, 149–158,

- 2007.
17. Hu, Y.-S., M. Li, G.-P. Gao, J.-S. Zhang, and M.-K. Yang, "A double-printed trapezoidal patch dipole antenna for uwb applications with band-notched characteristic," *Progress In Electromagnetics Research*, Vol. 103, 259–269, 2010.
 18. Ahirwar, S. D., Y. Purushottam, T. Khumanthem, and C. Sairam, "Wideband traveling wave Koch dipole antenna," *Progress In Electromagnetics Research C*, Vol. 18, 103–110, 2011.
 19. Karim, M. N. A., M. K. Abd Rahim, H. A. Majid, O. B. Ayop, M. Abu, and F. Zubir, "Log periodic fractal koch antenna for UHF band applications," *Progress In Electromagnetics Research*, Vol. 100, 201–218, 2010.
 20. Ramadan, M. H., K. Y. Kabalan, A. El-Hajj, S. Khouryand, and M. Al-Husseini, "A reconfigurable U-Koch microstrip antenna for wireless applications," *Progress In Electromagnetics Research*, Vol. 93, 355–367, 2009.
 21. Abbosh, A., "Accurate effective permittivity calculation of printed center-fed dipoles and its application to quasi Yagi-Uda antennas," *IEEE Transactions on Antennas and Propagation*, Vol. 61, No. 4, 2297–2230, 2013.
 22. Gao, S., S. Xiao, H. Zhu, W. Shao, and B.-Z. Wang, "2.45 GHz body-worn planar monopole antenna and its application in body-worn MIMO system," *Journal of Electromagnetic Waves and Applications*, Vol. 25, Nos. 5–6, 661–671, 2011.
 23. Gemio, J., J. Parron, and J. Soler, "Human body effects on implantable antennas for ISM bands applications: Models comparison and propagation losses study," *Progress In Electromagnetics Research*, Vol. 110, 437–452, 2010.
 24. Osman, M. A. R., M. K. A. Rahim, N. A. Samsuri, M. K. Elbasheer, and M. E. Ali, "Textile UWB antenna bending and wet performances," *International Journal of Antennas and Propagation*, Vol. 2012, Article ID 251682, 12 pages, 2012.
 25. Jalil, M. E., M. K. A. Rahim, N. A. Samsuri, M. A. Abdullah, and K. Kamardin, "Wetness experiment for compact CPW-fed ultra wideband antenna using textile material," *2012 IEEE Asia-Pacific Conference on Applied Electromagnetics (APACE)*, 298–301, 2012.